CHEMICAL ENGINEERING TRANSACTIONS
VOL. 84, 2021
A publication of AIDIC
The Italian Association of Chemical Engineering
Online at www.cetjournal.it
Guest Editors: Paolo Ciambelli, Luca Di Palma

ISBN 978-88-95608-82-2; **ISSN** 2283-9216

Templated Synthesis of Honeycomb-like TiO_2 for Supercapacitor Applications

Maria Sarno[a], Gennaro Gentile[b], Eleonora Ponticorvo[a*]

[a] Department of Physics "E.R. Caianiello" and Centre NANO_MATES (Research Centre for Nanomaterials and Nanotechnology at the University of Salerno) University of Salerno, Via Giovanni Paolo II, 132 - 84084 Fisciano (SA), Italy.
[b] Institute for Polymers, Composites and Biomaterials, National Research Council of Italy, Via Campi Flegrei 34, 80078 Pozzuoli, Italy.
eponticorvo@unisa.it

A facile and cost-effective procedure to synthesize honeycomb-like porous TiO_2, which exhibits specific capacitance of 0.2 F/cm^2 at 20 mV/s, was proposed. Scanning Electron Microscopy (SEM), thermogravimetric analysis (TG), UV/Vis, Fourier Transform Infrared Spectroscopy (FTIR), and X-ray diffraction (XRD) were employed for characterization. The electrochemical performances of the electrode were investigated in acidic solution.

1. Introduction

Nowadays, thanks to their unique properties, including high power density, small size, cost-effectivness, long cycle life, and good reversibility (Wang et al., 2013), supercapacitors have become one of the most essential and promising energy storage devices.
Supercapacitors have been used for several applications, e.g., hybrid electric vehicles, portable pacemakers, electronic devices, energy management, and back-up memory systems (Xia et al., 2012). The electrode materials largely govern the supercapacitor electrochemical performance; electrodes with ordered structural morphologies could potentially deliver high capacitance. Thus, the key solution is developing enhanced electrodes having a large surface area and optimized diffusion paths, required for electrons and ions to accomplish fast redox reactions.
For electrode materials, numerous transition metal oxides and conducting polymers have been used (Yang et al., 2012). Among them, TiO_2 has been recognized as one of the most promising candidates due to its cheapness, natural abundance, environmentally safe (green) properties, both thermal and chemical stability, low toxicity, unique physical properties, and polymorphisms (So et al., 2012).
On the other hand, a suitable porosity and a large surface area can highlight the intrinsic properties of TiO_2. An intriguing opportunity to synthesize porous structures consists of the use of plant skins (vegetable and fruit membranes) (Miao et al., 2010), exploiting the internal peel structure to obtain fascinating and useful materials. To obtain a very promising pseudocapacitive material, made up of a hierarchical porous assembly having: a honeycomb-like structure to ensure rapid ion diffusion; wettability and electron transfer; stability in acid; and, with excellent properties for proton absorption and incorporation, we report TiO_2 based electrode. The electrode was prepared in a tomato skin natural template.
Scanning Electron Microscopy (SEM), thermogravimetric analysis (TG), UV/Vis, Fourier Transform Infrared Spectroscopy (FTIR), and X-ray diffraction (XRD) were employed for characterization. The electrochemical performances of the electrode were investigated by cyclic voltammetry (CV) tests in an acidic solution. The results of CV measurements proved that the honeycomb-like TiO_2 based supercapacitor has good electrochemical capacitance performance within a wide potential range and improved electrochemical stability.

2. Experimental

2.1 Materials

Tomatoes (tomato is grown in the Campania region, Italy) were acquired from local markets on different dates. Hydrochloric acid (HCl), isopropyl alcohol, titanium(IV) isopropoxide ($Ti[OCH(CH_3)_2]_4$), sulfuric acid (H_2SO_4), Nafion 117 solution (5%) were acquired from Sigma-Aldrich and used without further purification. All of them were analytical grade.

2.2 Sample preparation

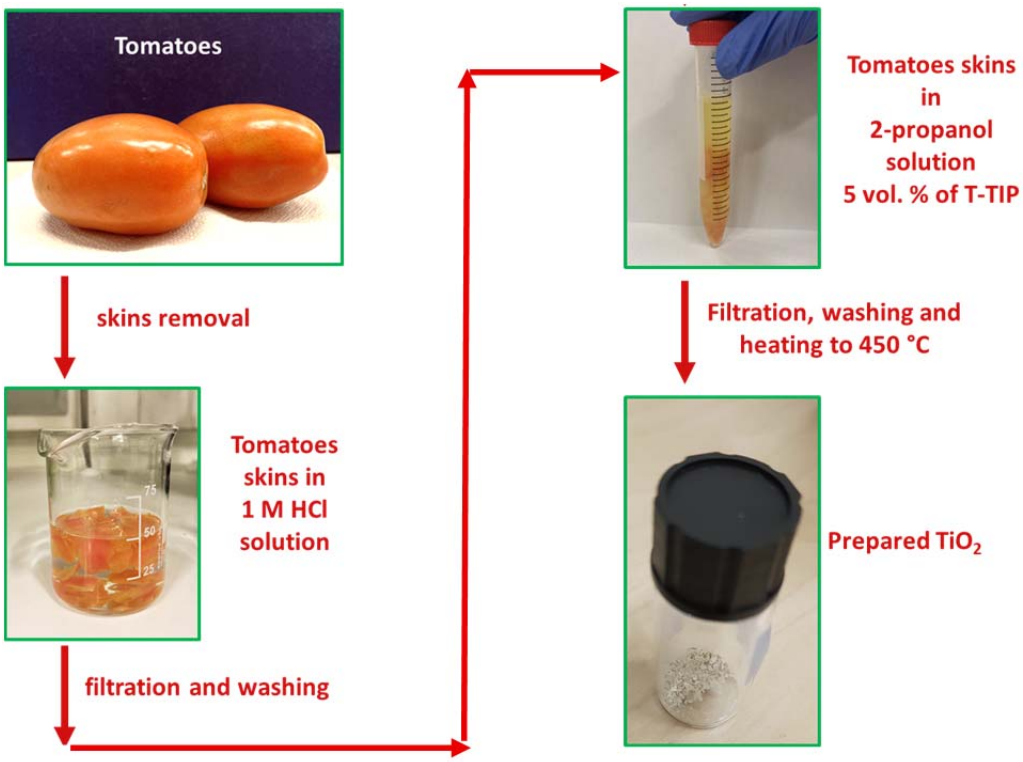

Figure 1: TiO_2 preparation scheme

For TiO_2 preparation, the proposed method was followed (Figure 1): (i) the outer tomatoes skins were hand detached and fragmented; (ii) the skins were washed with 1.5 mol/L HCl for 24 h; (iii) after filtration, the skins were washed with distilled water. For skin dehydration, tomato skins were rinsed with 2-propanol. Then, they were immersed in a 2-propanol solution 5 vol. % of TTIP (330 $\mu L_{TTIP}/g_{treated\ tomato\ skins}$), for fourteen hours. The addition of 25 mL of water followed. After two hours, the skins were filtered and rinsed with distilled water. Finally, the materials were treated at 450 °C for 5 h in an air atmosphere to remove all organics and favor titania crystallization.

2.3 Characterization methods

The characterization was obtained by the combined use of different techniques. Scanning electron microscopy (SEM) images were obtained by the use of a Tescan FIB-SEM, equipped with an energy dispersive X-ray (EDX) probe. A Bruker D8 X-ray diffractometer with a monochromatic CuKα radiation was used for measurements of powder diffraction profiles. The thermal behavior of the samples was investigated using thermogravimetric (TG) and derivative thermogravimetric (DTG) analysis (Mettler Toledo TGA, Model), between 25 and 1000 °C under air flow (60 mL min^{-1}) with a heating rate of 10 °C min^{-1}. FTIR was recorded on the Fourier transform infrared spectrometer BRUKER VERTEX-70, (Bruker Corporation). A Thermo Scientific Evolution 60S UV-Visible spectrophotometer was also used. The surface area was obtained by N_2 adsorption-desorption at 77 K (Kelvin 1042 V3.12, COSTECH Instruments). Electrochemical tests to evaluate capacitance performances of the synthesized samples, in particular cyclic voltammetry (CV) tests, were carried out by means of an Autolab PGSTAT302N potentiostat. For electrode preparation, 4 mg of TiO_2 were dispersed into 80 µl of a 5 wt% Nafion solution, 200 µl of ethanol and 800 µL of water (Sarno and Ponticorvo,

2020). The subsequent mixture consists of a homogeneous suspension which, after being sonicated for 30 mins and then air-dried, was partially deposited dropwise onto a Screen Printed Electrode (SPE) (Rowley-Neale et al., 2015; Sarno and Ponticorvo, 2018; Sarno et al., 2019). The Eq (1) was used to evaluate the sample specific capacitance:

$$C_{SP} = \frac{\int I \cdot dV}{\Delta V \cdot v} \quad (1)$$

ΔV is the voltage range, I is the current density, v is the CV scan rate.

3. Results and discussion

3.1 Chemical and morphological characterization

Figure 1 shows the X-ray pattern of the as-prepared sample, which can be assigned to a pure anatase TiO_2 phase (JCPDS 21-1272): the diffraction peaks at 24.71°, 37.24°, 47.32°, 53.13°, 54.45°, 61.17°, 62.56°, 69.91°, and 74.65° of 2θ correspond to (101), (004), (200), (105), (211), (213), (204), (116), and (215), respectively, of the TiO_2 anatase phase (Mihankhah et al., 2018; Cheng et al., 2019). At small angles, a broad band is observed, likely due to the sample holder. Low TiO_2 crystallinity is expected due to low temperatures sample preparation.

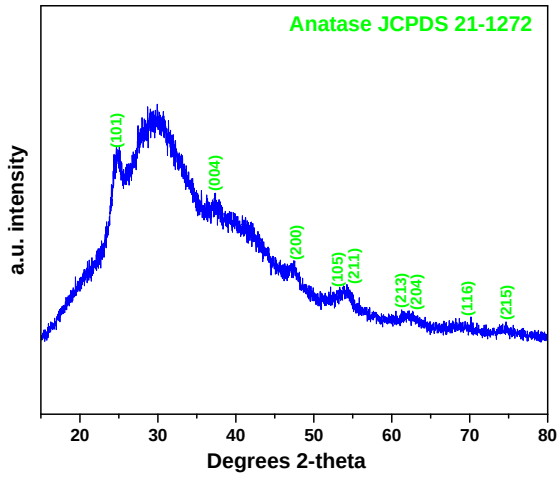

Figure 1: XRD pattern of TiO_2

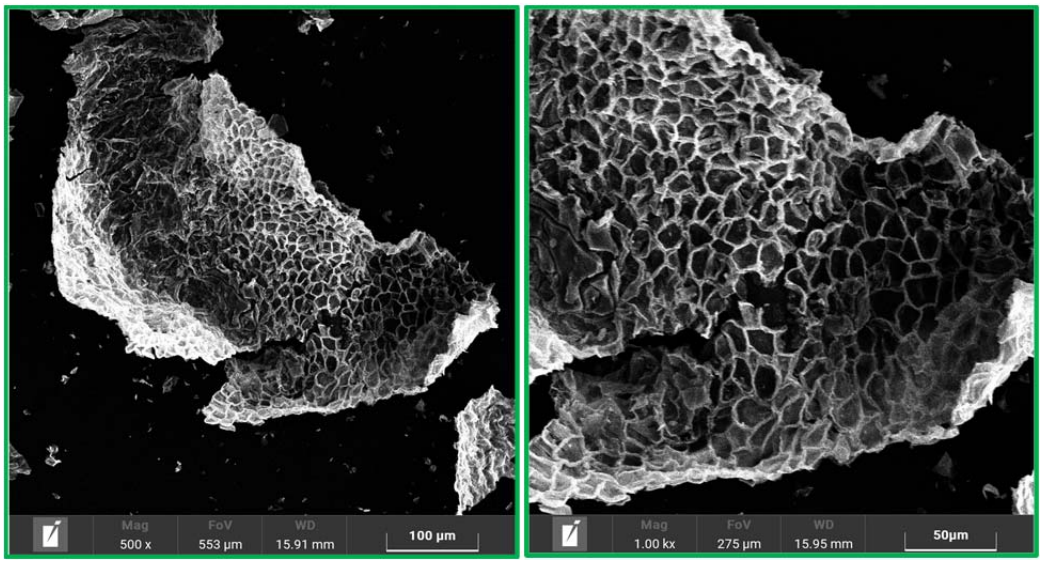

Figure 2: SEM images of TiO_2

The morphology of prepared material in the tomato skin template was characterized by scanning electron microscopy (SEM). As visualized in Figure 2, the TiO_2 nanosheet arrays were uniformly grown on the structure of tomato peels and interconnect with each other to form a honeycomb-like structure with a rough surface.
The porous nanosheet arrays with a rough surface can be expected to provide more reaction active sites and facilitate fast ion and electron transportation, which are beneficial for the enhancement of electrochemical performance (You et al., 2016). The specific surface area was determined by multiple point Brunauer-Emmett-Teller (BET) method in the region of the isotherm. A BET surface area of 52 m^2/g was obtained. The TiO_2 UV-VIS spectrum, collected in the wavelength (λ) range between 200 and 500 nm, is shown in Figure 3. Exciton absorption band maximum located at ~ 271 nm is very characteristic for the bandgap of anatase TiO_2, which is well known and widely reported (Barreca et al., 2010; Sugimoto et al., 2003; Iwabuchi et al., 2004).

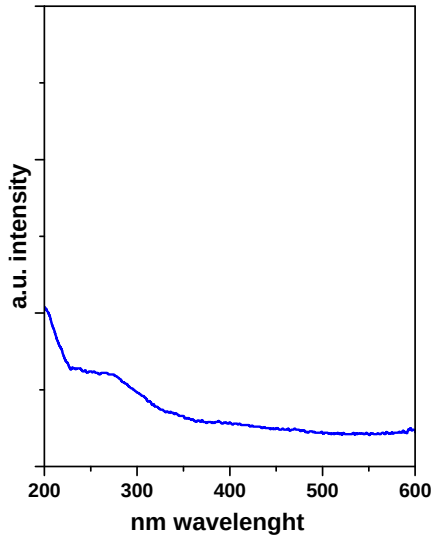

Figure 3: UV-vis absorption spectrum of TiO_2

The FTIR spectrum of TiO_2 prepared is shown in Figure 4. The broadband centered at 500-900 cm^{-1} is assigned to the bending vibration (Ti-O-Ti) bonds in the TiO_2 lattice (Hamadanian et al., 2010). The band at ~1611 cm^{-1} refers to the characteristic bending vibration of the -OH group (Vetrivel et al., 2015). The broadband centered at 3000-3500 cm^{-1} is assigned to the intermolecular interaction of hydroxyl group for water molecule with TiO_2 surface. TiO_2 TG-DTG profiles are shown in Figure 5; the decrease in weight up to 150 °C can be attributed to the desorption of physisorbed water (Nilchi et al., 2010). Subsequently, up to ~ 400 °C a weight loss due to organic residues release occurs. Above 400 °C, the variation in weight is very small.

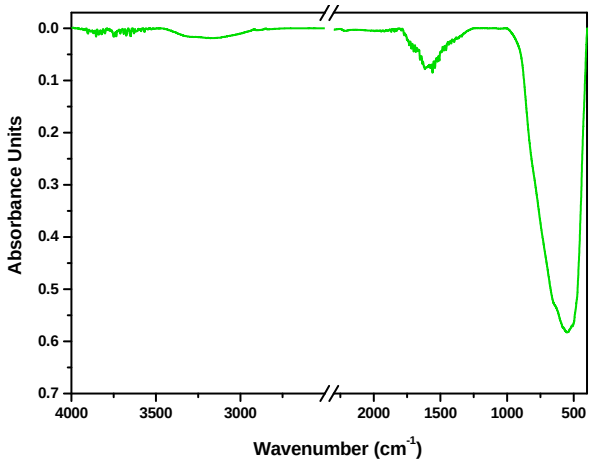

Figure 4: FT-IR spectrum of TiO_2

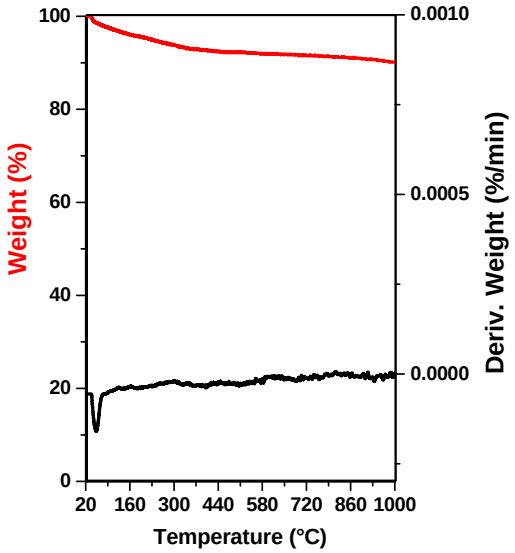

Figure 5: TG-DTG profile of TiO_2

3.2 Electrochemical characterization

CV curves at positive potentials vs. standard hydrogen electrode (SHE) of the prepared sample at different scan rates (2, 20, 50, 100, and 150 mV/s), in the potential range 0.05 ÷ 0.65 V in a 0.5 M H_2SO_4 electrolyte solution, were reported in Figure 6. As can be seen from the CV curves, the TiO_2 electrode exhibits a quasi-rectangular shape even at a high scan rate of 150 mV/s. No detectable redox peaks can be found in the chosen potential window, which indicates a nearly ideal capacitive behavior (Karandikar et al., 2012; Nishihara et al., 2012). The capacitance of 0.2 F/cm^2 was obtained thanks to the 3D interconnected porous structure (Senthilkumar et al., 2013), which plays an important role in electrochemical performance due to the easiness of electrolyte ions pass through the porous structure, improving wettability and leading to a good capacitance of the electrode. Moreover, long-term cycling experiments, in 0.5 M H_2SO_4 over 8000 cycles at 50 mV/s, were also performed showing that 97 % of the specific capacitance was retained.

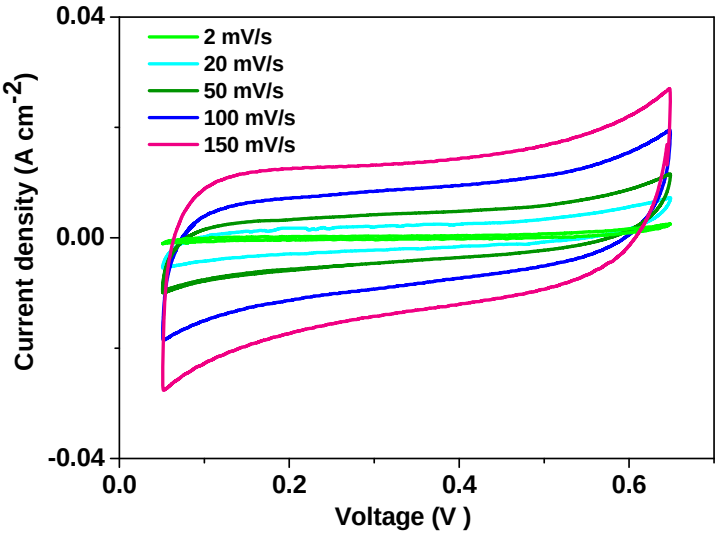

Figure 6: CV curves of TiO_2 at different scan rates

4. Conclusions

In summary, honeycomb-like TiO_2 structure with 3D highly interconnected pore structure, and plenty of micropores, was fabricated inside a natural plant skin. These superior structural parameters contribute to short diffusion paths and to rapid ions transport, as well as wettability and fast electron transport, which determine high electrochemical performances. This work leads to the development of promising TiO_2 based electrode materials for superior supercapacitors through a facile and economical preparation approach.

References

Barreca F., Acacia N., Barletta E., Spadaro D., Currò G., Neri F., 2010, Small size TiO_2 nanoparticles prepared by laser ablation in water, Applied Surface Science, 256, 6408–6412.

Cheng S., Gao Y.-J., Yan Y.-L., Gao X., Zhang S.-H., Zhuang G.-L., Deng S.-W., Wei Z.-Z., Zhong X., Wang J.-G., 2019, Oxygen vacancy enhancing mechanism of nitrogen reduction reaction property in Ru/TiO_2, Journal of Energy Chemistry, 39, 144–151.

Hamadanian M., Reisi-Vanani A., Majedi A., 2010, Sol-gel preparation and characterization of Co/TiO_2 nanoparticles: Application to the degradation of methyl orange, Journal of the Iranian Chemical Society, 7, S52–S58.

Iwabuchi A., Choo C.-K., Tanaka K.J., 2004, Titania Nanoparticles Prepared with Pulsed Laser Ablation of Rutile Single Crystals in Water, The Journal of Physical Chemistry B, 108, 10863–10871.

Karandikar P.B., Talange D.B., Mhaskar U.P., Bansal R., 2012, Development, modeling and characterization of aqueous metal oxide based supercapacitor, Energy, 40, 131-138.

Miao Y., Zhai Z., He J., Li B., Li J., Wang, J., 2010, Synthesis, characterizations and photocatalytic studies of mesoporous titania prepared by using four plant skins as templates, Materials Science and Engineering C, 30, 839–846.

Mihankhah T., Delnavaz M., Khaligh N.G., 2018, Application of TiO_2 nanoparticles for eco-friendly biodiesel production from waste olive oil, International Journal of Green Energy, 15, 69−75.

Nilchi A., Janitabar-Darzi S., Mahjoub A.R., Rasouli-Garmarodi S., 2010, New TiO_2/SiO_2 nanocomposites—Phase transformations and photocatalytic studies, Colloids and Surfaces A: Physicochemical and Engineering Aspects, 361, 25–30.

Nishihara H., Kyotani T., 2012, Templated nanocarbons for energy storage, Advanced Materials, 24, 4473-4498.

Rowley-Neale S.J., Brownson D.A.C., Smith G.C., Sawtell D.A., Kelly P.J., Banks C.E., 2015, 2D nanosheet molybdenum disulphide (MoS_2) modified electrodes explored towards the hydrogen evolution reaction, Nanoscale, 7, 18152–18168.

Sarno M., Ponticorvo E., 2018, Continuous flow HER and MOR evaluation of a new Pt/Pd/Co nano electrocatalyst, Applied Surface Science, 459, 105-113.

Sarno M., Ponticorvo E., Scarpa D., 2019, Ru and Os based new electrode for electrochemical flow supercapacitors, Chemical Engineering Journal, 377, 120050.

Sarno M., Ponticorvo E., 2020, Fe_3O_4/graphene electrode for the electrochemical detection of 4-ntrophenol, Chemical Engineering Transactions, 79, 427–432.

Senthilkumar S.T., Kalai Selvan R., Leeb Y.S., Melo J.S., 2013, Electric double layer capacitor and its improved specific capacitance using redox additive electrolyte, Journal of Materials Chemistry A, 1, 1086–1095.

So S., Lee K., Schmuki P., 2012, Ultrafast growth of highly ordered anodic TiO_2 nanotubes in lactic acid electrolytes, Journal of the American Chemical Society, 134, 11316–11318.

Sugimoto T., Zhou X., Muramatsu A.J., 2003, Synthesis of uniform anatase TiO_2 nanoparticles by gel–sol method: 3. Formation process and size control, Journal of Colloid and Interface Science, 259, 43–52.

Vetrivel V., Rajendran K., Kalaiselvi V., 2015, Synthesis and characterization of Pure Titanium dioxide nanoparticles by Sol- gel method, International Journal of ChemTech Research, 7, 1090-1097.

Wang Z., Ma C., Wang H., Liu Z., Hao Z., 2013, Facilely synthesized Fe_2O_3–graphene nanocomposite as novel electrode materials for supercapacitors with high performance, Journal of Alloys and Compounds, 552, 486–491.

Xia X., Hao Q., Lei W., Wang W., Sun D., Wang X., 2012, Nanostructured ternary composites of graphene/Fe_2O_3/polyaniline for high-performance supercapacitors, Journal of Materials Chemistry, 22, 16844–16850.

Yang W., Gao Z., Wang J., Wang B., Liu Q., Li Z., Mann T., Yang P., Zhang M., Liu L., 2012, Synthesis of reduced graphene nanosheet/urchin-like manganese dioxide composite and high performance as supercapacitor electrode, Electrochimica Acta, 69, 112–119.

You Y., Yao H.R., Xin S., Yin Y.X., Zuo T.T., Yang C.P., Guo Y.G., Cui Y., Wan L.J., Goodenough J.B., 2016, Subzero-temperature cathode for a sodium-ion battery, Advanced Materials, 28, 7243–7248.